

Hotspot temperature analysis of distribution transformer under unbalanced harmonic loads using finite element method

Muhammad Haziq Mohd Wazir^{1,2}, Dalila Mat Said^{1,2}, Zaris Izzati Mohd Yassin³,
Siti Aisyah Abd Wahid¹

¹Centre of Electrical Energy Systems, Institute of Future Energy, Universiti Teknologi Malaysia, Johor Bahru, Malaysia

²Faculty of Electrical Engineering, Universiti Teknologi Malaysia, Johor Bahru, Malaysia

³School of Engineering and Computing, Manipal International University, Nilai, Malaysia

Article Info

Article history:

Received Jul 10, 2023

Revised Sep 19, 2023

Accepted Dec 13, 2023

Keywords:

Distribution transformer

Harmonic distortion

Hot spot temperature

Finite element method

Insulation temperature class

ABSTRACT

In an electrical power distribution system, harmonic distortion is the most prominent power quality problem that causes long-term adverse effects such as failure of distribution transformers. Considering that most transformer problems are caused by heat losses due to the presence of harmonics, it was decided to use a numerical method with the highest accuracy, finite element method (FEM) to analyze the hot spot temperature (HST) of the thermal distribution transformer model. Through the use of COMSOL Multiphysics software, three phases of unbalanced harmonic loads are considered, which contribute to three different total harmonic distortion current (THDI) levels and five different insulation temperature classes. Using the IEEE C57.110-2018 guidance, the simulation outputs are then verified with HST results from the HST mathematical model. The findings indicated that with the increased loadings, the unbalanced harmonic currents have impacted the HST increment and distinguished the HST values between the phases.

This is an open access article under the [CC BY-SA](https://creativecommons.org/licenses/by-sa/4.0/) license.



Corresponding Author:

Dalila Mat Said

Faculty of Electrical Engineering, Universiti Teknologi Malaysia

Johor Bahru, 81310, Malaysia

Email: dalila@utm.my

1. INTRODUCTION

Malaysia, as a developing nation, has not been alone in utilizing power electronics technologies to enhance its own system in support of the country's development ever since they were developed to replace the conventional alternating current (AC) electrical system. In light of this, it is anticipated that electricity power will be drawn along the distribution networks of high quality. Unfortunately, undesirable power quality events like harmonics prevented the power from reaching its ideal state. The most common issue with electrical power distribution network power quality is harmonic distortion. Harmonics were defined as integer multiples of the fundamental line frequency by international standard bodies like the Institute of Electrical and Electronics Engineers (IEEE).

The electrical distribution equipment's nonlinear loads, which are primarily responsible for frequency variations, were the primary source of the harmonics. The steady-state wave shape of a nonlinear load is defined as not following the wave shape of the applied voltage [1]. In addition to the distorted power sinusoidal wave shape, nonlinear harmonic loads may also cause power losses to rise, overheating the distribution transformer, poor power factor conditions that force users to pay a penalty, disruptions in the smooth operation of large-scale production at industrial sites, and numerous other irritating network issues.

A distribution transformer is an essential component of the distribution system in any electrical system network. It enables the utility provider to deliver power to its customers. It supplies voltage to the

electricity consumer via four wire cables, which typically require a high demand supply. As a result, the electricity delivery system's most expensive piece of equipment is the distribution transformer. In light of this, it is crucial to preserve the distribution transformer's best performance while also maintaining its durability and lifetime expectancy. To avoid a significant loss as a result of the transformer breaking down, it is best to explain the potential root cause of any potential failure at an earlier stage. Singh and Singh [2] stated that the most common reason for distribution transformer failure was excessive heat on the transformer. The group of previous studies, which mostly agreed that heat is the primary cause of the distribution transformer's failure [3]–[10], strongly support this assertion. In addition, the authors discovered that the low voltage (LV) side winding of the transformer experiences more failures than the transformer's core or other components. The winding insulation's deterioration is said to frequently cause failure elsewhere [11]–[14]. On the other hand, numerous literatures have stated that harmonic currents are the root of excessive heat generation on the distribution transformer winding [15]–[20]. Although several works have explored the impact of harmonics on the distribution transformer, it appears that the impact of harmonic level variations on the HST behavior was not specifically addressed in previous works. Most of the existing studies concentrated only on the higher value of total harmonic distortion current (THDI) instead of considering the lower values [21]–[26]. Moreover, the harmonic current behavior towards the hot spot temperature (HST) should be analyzed according to the specific load levels at a particular time. Therefore, a comprehensive analysis is needed to identify the impact of harmonic current load from different levels on the HST behavior on the LV windings of distribution transformer.

Therefore, this paper examines the HST behavior on the LV windings of distribution transformer, by employing different THDI levels from separated times of five different insulation temperature classes of distribution transformer. The measured and collected data for this research mainly came from detected problematic transformers at substations that supply to commercial load buildings. The HST analysis is carried out using FEM using COMSOL Multiphysics software. The validation of the findings is then conducted by comparing the simulation results with the HST mathematical model using IEEE approach.

2. METHOD

This section provides an overview of the methodology applied in this research. This section includes aspects like data specifications for distribution transformers, clarification of the rated values for hot spot temperatures in accordance with established standards, mathematical formulation involved in the research works, modelling of thermal distribution transformers, and the evaluation method, all based on the approached mentioned. A detailed analysis is provided in the discussion that follows, which is presented in several subsections.

2.1. Distribution transformer specification data

The cast resin transformer, also known as a dry type of transformer, is the type of transformer being used in this study. As a result, the genuine field measurement data were gathered from the problematic substation that was found and supplies voltage to the commercial buildings nearby. The power analyzer software is used for online monitoring of the measurement. Table 1 shows the details of that particular distribution transformer's specifications.

Table 1. Distribution transformer data specification

Specification	Value
Sizing	500 kVA
Primary voltage	22 kV
Secondary voltage	433 V
Primary current	13.1 A
Secondary current	667 A
Frequency	50 Hz
Maximum rated ambient temperature	40 °C
Ambient temperature	30 °C
Winding material	Copper (Cu)

2.2. Rated hot spot temperature of distribution transformer

To analyze the impact from the unbalanced harmonic loads towards the transformer, the rated hotspot temperatures, $\theta_{HS-rated}$ for the distribution transformer are determined by the insulation temperature classes all five types of the insulation temperature classes of 130 °C, 150 °C, 180 °C, 200 °C and 220 °C are used to determine the $\theta_{HS-rated}$ by each class in this research. According to [27], the $\theta_{HS-rated}$ is 10 °C less

than a temperature class, based on a 30 °C ambient temperature. In this regard, this $\theta_{HS-rated}$ is also named as temperature rise limit in the standard. In this case, the temperature rise limit is focused on the specified LV winding parts of this 500 kVA distribution transformer. Typically, the $\theta_{HS-rated}$ value of the transformer is determined by the manufacturer who designs and construct the transformer. However, since the primary objective of this study is to determine any particular hotspot temperature value that has exceeded the limit, therefore the best technique is by taking the maximum temperature rise limit as the rated hotspot value. Thus, according to the mentioned standard, the maximum hottest-spot rated temperature in Table 2 is referred to as the rated hotspot temperature value for the distribution transformer, which is also referred for the HST compliance check and determination of the premature failure condition inside the transformer.

Table 2. Temperature rise limits over ambient temperature for dry-type distribution transformer

Insulation system temperature class (°C)	Maximum hottest-spot rated temperature (°C)	Maximum hottest-spot rated temperature, loading above rating for resin-encapsulated transformer (°C)
130	120	200
150	140	220
180	170	250
200	190	270
220	210	290

2.3. Total harmonic distortion current (THDI) range classification

The harmonic current data is collected from a substation transformer supplying a commercial load building. In this case, the classification of THDI range is based on the collected harmonic current load data from three different working hours in the same day considering different active operation period of the LV network. The three different working hours are categorized based on peak hour, average hour and low hour. Therefore, the range of the THDI collected for each level is classified as shown in Table 3.

Table 3. THDI range classification

THDI level	Time	THDI range (%)
Peak	4:20 pm	19% < THDI < 22%
Average	12:30 pm	16% < THDI < 18%
Low	14:10 pm	12% < THDI < 15%

2.4. Harmonic loss correction calculation

The indication of harmonic current impact on the winding temperature rise can be expressed through the evaluation of eddy current losses. Therefore, the collected harmonic loads data from the LV side of distribution transformer are utilized to quantify their harmonic loss factor, FHL_{ec} , as expressed in (1), indicating the influence of harmonic to the eddy current losses which is actively generated on the LV winding part of the distribution transformer. Based on the written expression, I_h represents the harmonic current component, I_1 is the fundamental current and h is the harmonic order. Meanwhile, the corrected losses for due to the harmonic loss factor is expressed as in (2), where P_0 is the corrected eddy current losses, P_{ec} is the eddy current losses, and FHL_{ec} is the eddy current harmonic loss factor.

$$FHL_{ec} = \frac{\sum_{h=1}^{h=\max} \left(\frac{I_h}{I_1}\right)^2 h^2}{\sum_{h=1}^{h=\max} \left(\frac{I_h}{I_1}\right)^2} \quad (1)$$

$$P_0 = FHL_{ec} P_{ec} \quad (2)$$

2.5. Thermal distribution transformer modelling for HST analysis

The FEM analysis approach is split into two parts which were modeling the two-dimensional cross section of the transformer and simulating the designed model with the harmonic composition from the site's data collection. For modeling part, the FEM COMSOL software is utilized to simulate the thermal model in a finite element environment. Figure 1 depicts the dry type of distribution transformer's cross section for the three-phase 500 kVA load. The transformer model is portrayed as single-phase based on the presumption that the design of each winding of the three-phase transformer is physically similar. As a result, it has the potential to simplify the geometry design that must be assembled in order to achieve the desired result. There are three sets of materials used in this model: copper for the transformer LV winding domain as shown in the

red circle in Figure 2, iron for the transformer core domain as shown in the red rectangle in Figure 3 and air for the coolant domain as shown in the green region in Figure 4. Table 4 shows that each type of material has its own set of properties.

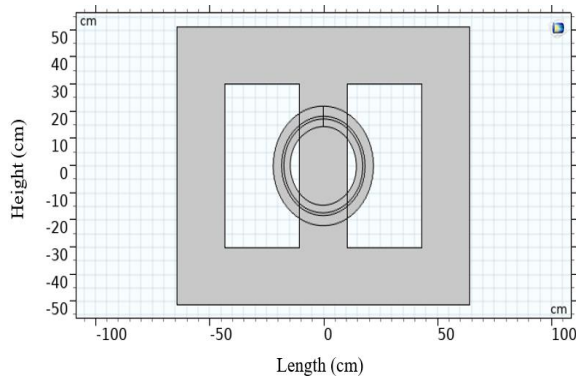


Figure 1. The 2D cross section of the dry-type geometry transformer model

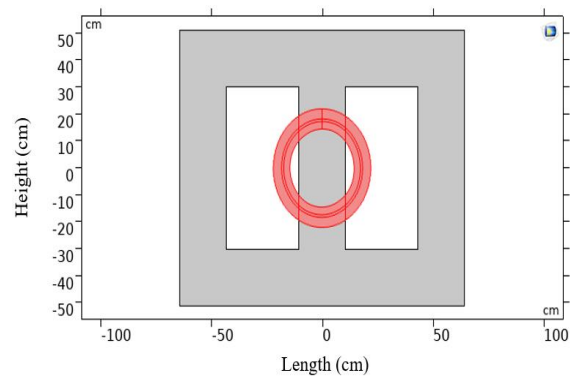


Figure 2. The copper material for the LV winding domain of the transformer

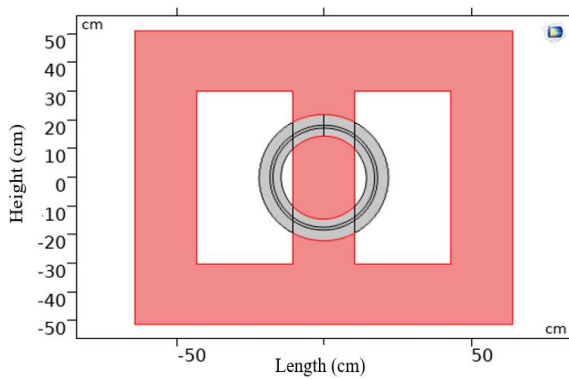


Figure 3. The iron material for the core domain of the transformer

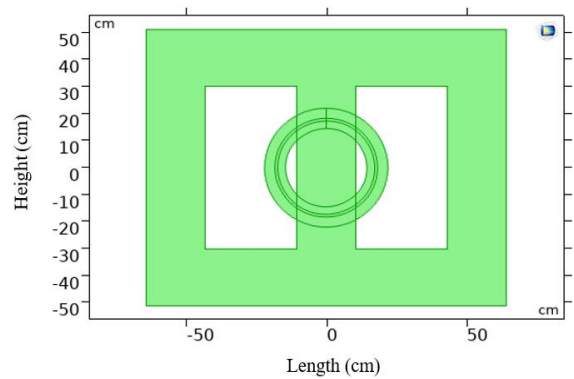


Figure 4. The air material for the coolant domain of the transformer

Table 4. Material properties for copper, iron and air

Property	Copper	Iron	Air
Relative permeability, μ_r	1	4,000	1
Electrical conductivity, σ	5.998e7 S/m	1.12e7 S/m	0 S/m
Heat capacity at constant pressure, C_p	385 J/(kg.K)	440 J/(kg.K)	Overrides copper and iron material
Relative permittivity, ϵ	1	1	1
Density, ρ	8,940 kg/m ³	7,870 kg/m ³	Overrides copper and iron material
Thermal conductivity, k	400 W/(m.K)	762 W/(m.K)	Overrides copper and iron material

2.6. The heat source allocation on LV winding

As shown in Figure 5, the green spot represents the heat source, Q which is applied specifically on the LV winding region, expressed in (3). The heat rate of the power losses, P_0 over a volume, V which expressed in (4), and encompassed the entire selected domain of the LV winding [28], defines the heat source. The corrected power losses, P_0 is equivalently known as the eddy current losses, are the effects of the three groups of harmonic distortion that were present in the three-phase unbalanced harmonic loads.

$$Q = Q_0 \quad (3)$$

$$Q_0 = \frac{P_0}{V} \quad (4)$$

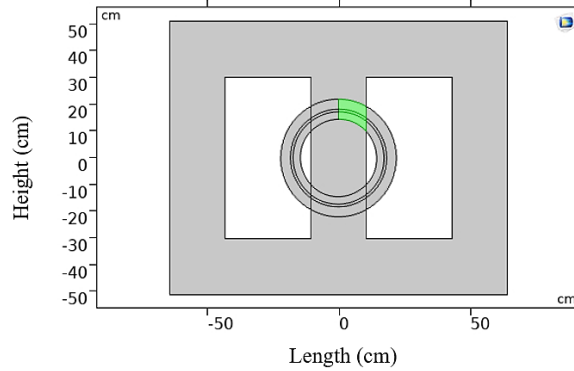


Figure 5. The heat source domain of the LV winding

2.7. Heat transfer and electromagnetic heating formulation

Once the above-mentioned settings are accomplished, the thermal distribution transformer model is then simulated with the heat transfer equation coupled with the Multiphysics solution of electromagnetic heating in order to gain the HST result value. It is important to note that the heat transfer simulation is specifically performed on the mentioned designed specific location of the LV winding. Therefore, the mathematical formulation of the heat transfer and the electromagnetic heating are expressed in (5) and (6) and (7) respectively [28].

$$d_z \rho C_p \frac{\partial T}{\partial t} + d_z \rho C_p u \cdot \nabla T + \nabla \cdot q = d_z Q + q_0 + d_z Q_{ted} \tag{5}$$

$$q = -d_z k \nabla T \tag{7}$$

$$\rho C_p \frac{\partial T}{\partial t} + \rho C_p u \cdot \nabla T = \nabla \cdot (k \nabla T) + Q_e \tag{8}$$

where d_z is the thickness of the geometry which had been uniformly set to 1 metre, ρ is the density, C_p is the specific heat capacity at constant pressure, u is the thermal heat coefficient, T is the temperature, q is the conductive heat flux, Q is the heat source, q_0 is the convection heat flux, k is the thermal conductivity. Meanwhile, Q_{ted} is the thermo elastic damping value which is often being neglected in practical. Lastly, Q_e represents the electromagnetic heat source.

2.8. HST evaluation region of thermal transformer model

Regarding the HST evaluation, it is being studied on the selected region of the cross section of the transformer model. The indication of red spot in Figure 6 represents the expected abnormal temperature rise region which will be evaluated for the HST study. The primary objective of this region selection is to analyze the rise in the HST of the LV winding which had been significantly inserted with the heat source, Q from the loads resulting from the harmonic composition. Then, the compliance of the HST is indicated throughout the simulation of this heat transfer study by referring to the above-mentioned standard.

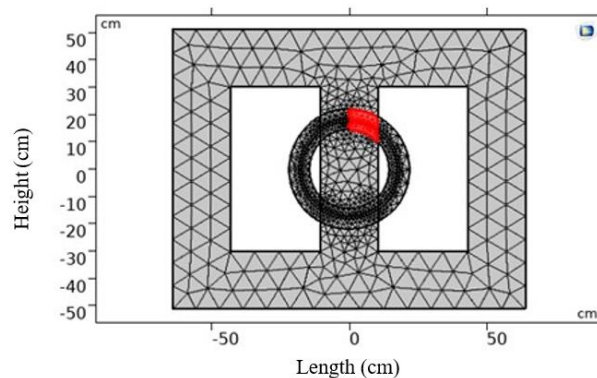


Figure 6. HST evaluation region of the thermal distribution transformer model

2.9. HST mathematical model using IEEE approach

The main IEEE standards that are used as references to validate the HST analysis of the thermal transformer model, especially for the dry-type distribution transformer, are IEEE Std C57.96-2013 and IEEE Std C57.110-2018. Besides, MATLAB's Simulink toolbox is used to construct the distribution transformer's HST mathematical model. The general mathematical expression of the total HST is shown in (8) due to the fact that this study is solely executed on the LV winding [29].

$$\theta_{HS} = \theta_a + \Delta\theta_{HS} \quad (8)$$

where the θ_{HS} is the hottest-spot winding temperature, θ_a is the ambient temperature and $\Delta\theta_{HS}$ is the hottest-spot temperature rise over ambient. All the temperatures are calculated in degree Celsius unit, °C. Meanwhile, the $\Delta\theta_{HS}$ is considered as a function of load for steady-state conditions and self-cooled operation. Hence, the mathematical expression to calculate the value of $\Delta\theta_{HS}$ is shown in (9) [29].

$$\Delta\theta_{HS} = \Delta\theta_{HS,r} \times [L]^{2m} \quad (9)$$

where $\Delta\theta_{HS,r}$ is the rated hottest-spot temperature rise over ambient at 1.0 per unit load, L is the per unit load and m is an empirical constant which the value is set to 0.8. The HST results at the LV winding along the transformer's loading, which ranged from 0.1 p.u. to 0.9 p.u., become the primary focus of the validation for each phase of the transformer cables, each THD group, and each insulation class. The plotted graphs that contain the comparison results from both approaches are then depicted and analyzed only when the HST from both approaches is validated. The HST compliance with the limit, the harmonic content that contributed to the HST, and the HST behavior along the transformer loading were all part of the analysis.

3. RESULTS AND DISCUSSION

In order to validate the findings, the simulation HST results from the FEM thermal distribution model are compared to the HST results obtained from the IEEE HST mathematical model. This section shows the comparison of HST results from both methods in every insulation temperature class. Each subsection illustrates another three HST comparison result from FEM thermal distribution model with the IEEE HST mathematical model for the THDI-peak-level (19%-22%), THDI-average-level (16%-18%) and THDI low-level case (12%-15%).

3.1. Validation for 130 °C insulation temperature class

Figure 7 shows HST simulation results between both mentioned approaches for THDI peak-level, average-level and low-level in 130 insulation temperature class. Based on Figure 7(a), it can be seen that the HST from the THDI peak-level case is obviously higher compared to other THDI levels, and it had crossed the maximum hottest spot temperature limit of 120 °C right before 0.7 pu in the phase B with the HST values of 126.31 °C, while 114.80 °C, and 114.02°C in each of phase A and phase C respectively. The final HST values at 0.9 pu from this THDI level are 159.29 °C, 176.31 °C and 158.12 °C, which all have surpassed the limit. Meanwhile, Figure 7(b) represents the THDI for average-level case, the HST had only reached the mentioned limit at 0.9 pu in phase B and phase C with the HST values of 123.27 °C and 130.56 °C respectively, while 118.39 °C in phase A. On the contrary, the HST values in THDI low-level are detected to remain under the limit for entire loading with the final HST values of 103.60 °C, 93.63 °C and 89.11 °C in phase A, phase B and phase C correspondingly as in Figure 7(c). Therefore, it can be clarified that the harmonic current load in this level is complying with the standard and will not put the transformer at any risk. The graphs vividly show the close similarity between the simulated HST values. The simulated HST values from both approaches are 96.3%, 98.9% and 99.7% in similarity for each THDI peak-level, THDI average-level and THDI low-level respectively.

3.2. Validation for 150 °C insulation temperature class

The results of validation for 150 °C are illustrated in Figure 8. Based on Figure 8(a), the HST from the THDI peak-level case is higher than the two other THDI levels. The HST in phase B has reached the maximum hottest spot temperature limit of 140 °C from the 0.7 pu onwards with the HST value of 144.25 °C, while 132.58 °C and 134.16 °C have resulted in phase A and phase C respectively. The final HST values from this THDI level are 176.22 °C, 192.89 °C and 178.55 °C at 0.9 pu. Meanwhile, the HST in THDI average-level is illustrated in Figure 8(b) that the HST values at 0.7 pu are far under the limit with 108.26 °C, 114.54 °C and 118.07 °C in phase A, phase B and phase C respectively. Only when

they reach at the 0.9 pu onwards, all the three phases are indicated to cross the 140 °C, with each HST valued at 141.56 °C, 151.28 °C and 156.21 °C accordingly. On the other hand, Figure 8(c) portrayed the HST values from THDI low-level which comply with the limit throughout the loading similarly as in the previous 130 insulation temperature class. The graphs clearly show the close similarity between the simulated HST values, notably at THDI average-level and THDI low-level case. The simulated HST values from both approaches in this class are 96.13%, 98.7% and 98.64% in similarity by each THDI level accordingly.

3.3. Validation for 180 °C insulation temperature class

The HST from 180 °C insulation temperature class is shown in Figures 9 for each THDI level. As for THDI peak-level, the HST values that crossed the maximum hottest spot temperature limit of 170 °C for this class are similarly happened in phase B from the 0.7 pu onwards with the HST value of 177.57 °C, while Phase A and Phase C each at 162.56 °C and 161.52 °C respectively. The final HST values from this THDI level are 218.97 °C, 239.59 °C and 217.54 °C at 0.9 pu as shown in Figure 9(a). Meanwhile the HST in THDI average-level, it can be seen in Figure 9(b) that the HST has only reached the mentioned limit by all phases at 0.9 pu, with the HST values of 174.74 °C, 183.13 °C and 189.35 °C in phase A, phase B and phase C respectively. On the other hand, the HST in the THDI low-level is observed to similarly remain under the limit along the loading as in the previous 130 and 150 insulation temperature classes, which are portrayed in Figure 9(c). The HST simulation results between both mentioned approaches for THDI peak-level, average-level and low-level in 180 insulation temperature class are compared. The graphs vividly show the close similarity between the simulated HST values, also notably at THDI average-level and THDI low-level case. The simulated HST values from both approaches in this class are illustrated in where it indicated 95.4%, 98.5% and 98.6% in similarity by each THDI level accordingly.

3.4. Validation for 200 °C insulation temperature class

Figure 10 represents the HST results for the insulation temperature class of 200 °C. The HST value in the peak level surpassed the maximum hottest spot temperature limit of 190 °C for this class at the 0.7 pu load. At this point, the HST in phase B has reached the limit with 193.63 °C, while closely followed by 180.57 °C, and 179.39 °C in phase A and phase C respectively. The final HST value from this THDI level is 244.63 °C, 262.39 °C and 243 °C at 0.9 pu as indicated in Figure 10(a). Meanwhile the HST in THDI average-level, it can be seen in Figure 10(b) that the HST in phase C has reached the mentioned limit at 0.9 pu with the HST value of 195.26 °C, while the HST in phase B and phase C are each at 179.40 °C and 180.32 °C. Lastly for THDI low-level in Figure 10(c), all HST values along the entire loading are detected to be safely complied to the limit, similarly as in the previous 130, 150 and 180 insulation temperature classes. The HST simulation results between both approaches for THDI peak-level, average-level and low-level in 200 insulation temperature class are compared. Even though there are results deviations in THDI average-level case, it still holds strong agreement between those results with 93.4% in similarity. Meanwhile, the simulated HST values in THDI peak-level and THDI low-level remained highly validated with 96.3%, and 97% in similarity for respective THDI levels.

3.5. Validation for 220 °C insulation temperature class

The HST results for 220 °C insulation temperature class are illustrated in Figure 11. As for THDI peak-level in 220 °C insulation temperature class in Figure 11(a), a bit difference in the HST behavior is observed, compared to other previous classes. At 0.7 pu, the HST values remained complying the maximum hottest spot temperature limit of 210 °C and merely approached the limit in phase B with the HST value of 209.48 °C, while phase A and phase C each at 198.29 °C and 196.97 °C respectively. The final HST values from this THDI level are 269.85 °C, 284.88 °C and 268.03 °C at 0.9 pu, which have surpassed the aforementioned limit. Meanwhile the HST in THDI average-level, it showed that the HST have only reached the mentioned limit by all phases at 0.9 pu, with the HST values of 210.69 °C, 211.39 °C and 215.88 °C in phase A, phase B and phase C respectively, which can be observed in Figure 11(b). Meanwhile in Figure 11(c), the HST in the THDI low-level is observed to similarly remain under the limit along the loading as in the previous 130, 150, 180 and 200 insulation temperature classes. The simulation results between both mentioned approaches for THDI peak-level, average-level and low-level in 220 insulation temperature class are shown. The graphs distinctly show the close similarity between the simulated HST values, notably at THDI peak-level and THDI low-level case. The simulated HST values from both approaches are 97.3%, 96.4% and 98% in similarity for each THDI peak-level, THDI average-level and THDI low-level respectively.

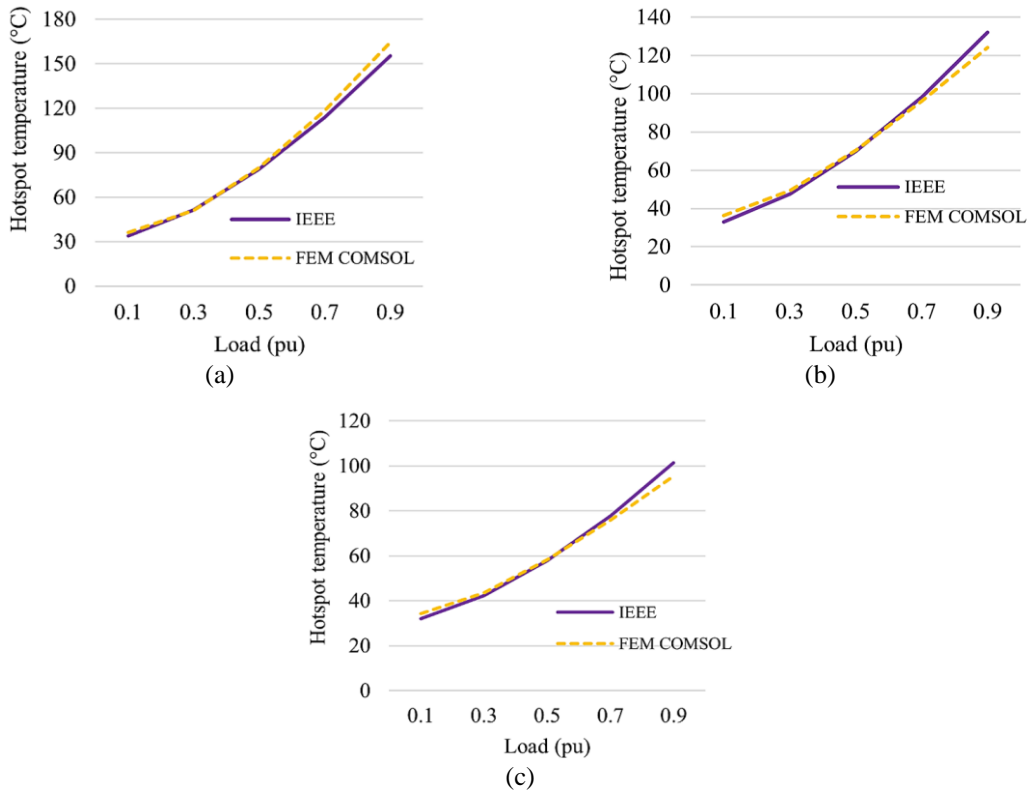


Figure 7. Comparison in FEM and IEEE approach for THDI peak-level, (a) THDI average-level, (b) THDI low-level, and (c) for 130 insulation temperature class

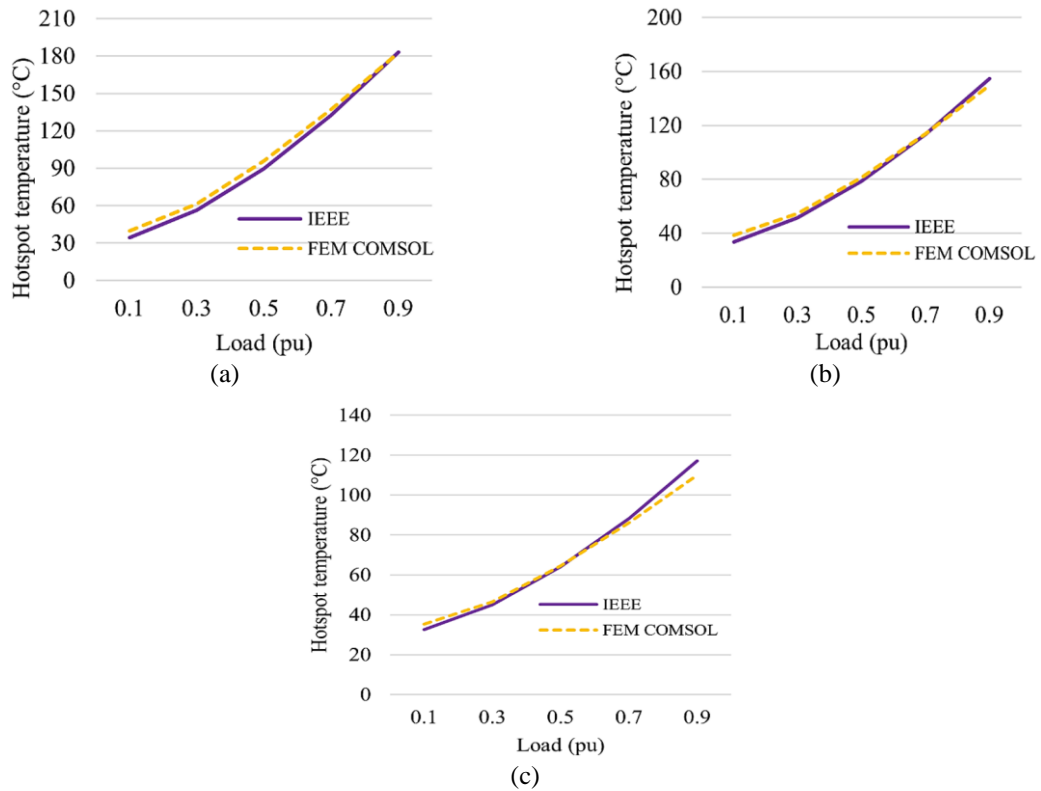


Figure 8. Comparison in FEM and IEEE approach for THDI peak-level, (a) THDI average-level, (b) THDI low-level, and (c) for 150 insulation temperature class

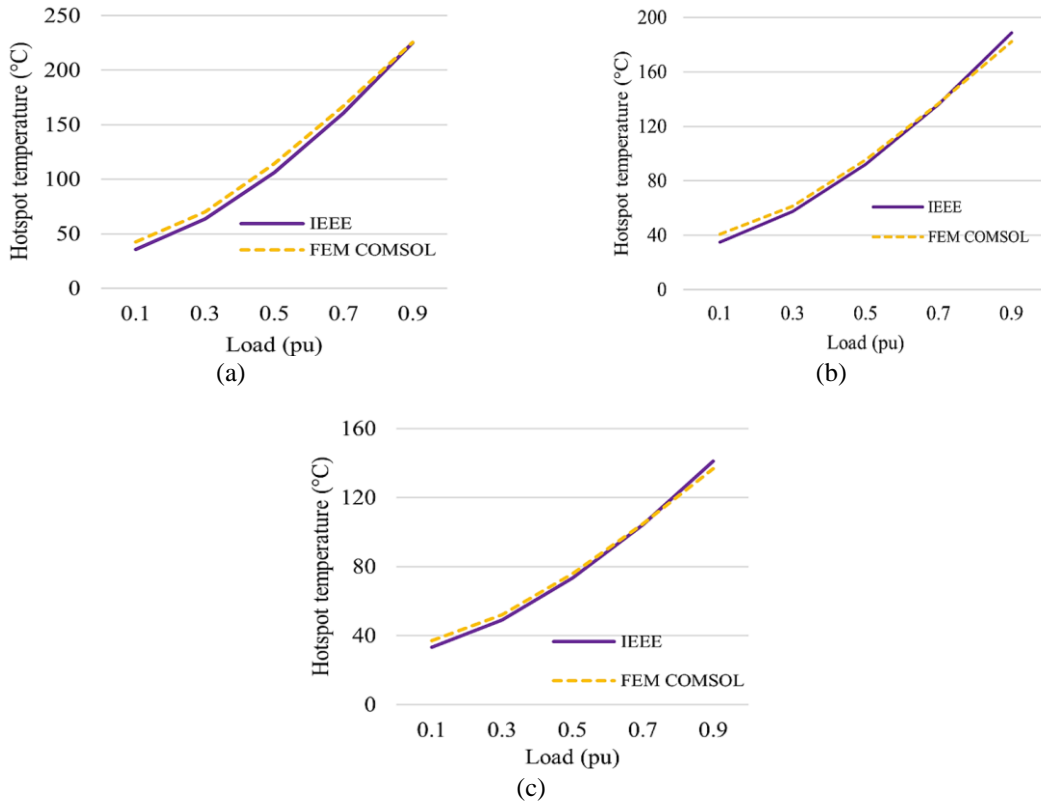


Figure 9. Comparison in FEM and IEEE approach for THDI peak-level (a) THDI average-level, (b) THDI low-level, and (c) for 180 insulation temperature class

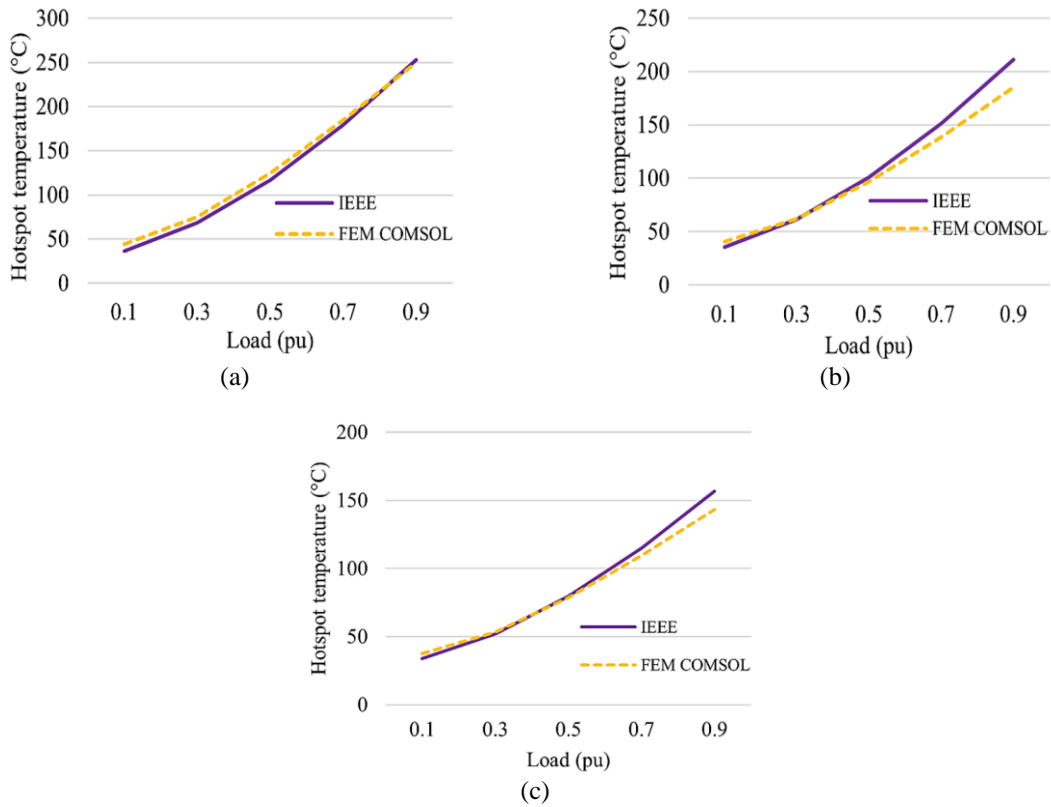


Figure 10. Comparison in FEM and IEEE approach for THDI peak-level, (a) THDI average-level, (b) THDI low-level, and (c) for 200 insulation temperature class

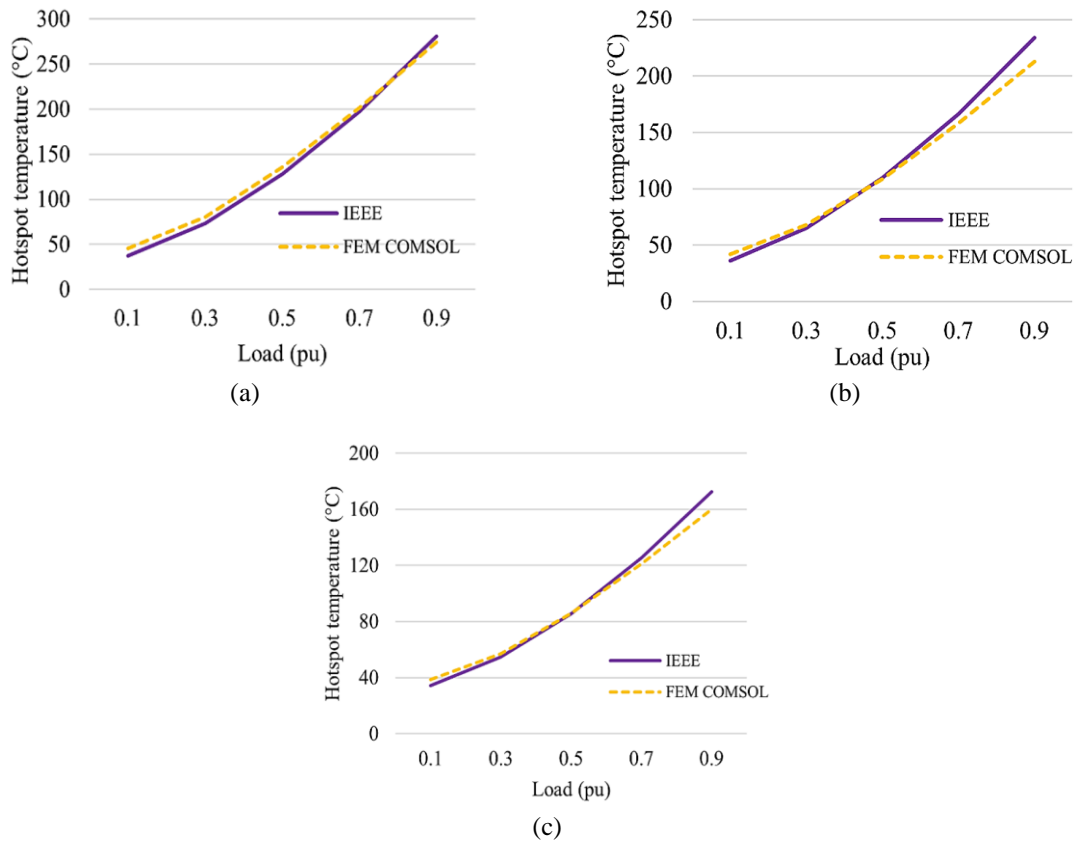


Figure 11. Comparison in FEM and IEEE approach for THDI peak-level, (a) THDI average-level, (b) THDI low-level, and (c) for 220 insulation temperature class

4. CONCLUSION

The study aims to observe and analyze the hot spot temperature behavior under different THDI levels and insulation temperature classes which may lead to the premature failure condition of the distribution transformer. Therefore, based on the obtained result, it is possible to conclude that if the transformer in this real case study is using all types of insulation temperature classes, the unbalanced harmonic current loads are not affecting the temperature and the HST is consistently complying with the standard regardless the level of the THDI. This is due to the reason that the transformer had very light loads during the measurement of harmonic currents. However, when the HST model is simulated for the case if the loading of the transformer is increasing, the measured unbalanced harmonic currents then started to impact the increment of the HST and distinguish the HST values between the phases. Furthermore, the differences in HST values are matched with the measured THDI by each phase from each THDI level as depicted earlier. Hence, the resulting HST in phase B, phase C and phase A of the THDI peak-level are significantly different and higher compared to the other two phases, average-level and low-level THDI. The potential cause could be the active operation of harmonic-generating equipment, which created a greater harmonic current in that specific phase compared to other phases. Another conclusion is that the uniform patterns are traced throughout the study for the entire HST simulation results from each insulation temperature class. Every HST simulation results in every class indicated compliance to the standard limit up to 0.9 pu. Apart from that, when the transformer loading is above the rating limit for THDI peak-level in the 200 and 220 insulation temperature classes, the HST gets closer to exceeding the maximum hottest spot temperature limit. This demonstrated the importance of choosing the right insulation temperature class for the distribution transformer based on the transformer's size and the loads that will be supplied.

ACKNOWLEDGEMENTS

This paper was developed in the laboratories of Centre of Electrical Energy Systems, CEES, Faculty of Electrical Engineer, Universiti Teknologi Malaysia (UTM) and funded by the Ministry of Higher Education under FRGS, Registration Proposal No: FRGS/1/2021/TK0/UTM/02/12.

REFERENCES

- [1] R. Langella, A. Testa, and E. Alii, "IEEE recommended practice and requirements for harmonic control in electric power systems," *IEEE Recommended Practice*, 2014.
- [2] R. Singh and A. Singh, "Causes of failure of distribution transformers in India," in *2010 9th International Conference on Environment and Electrical Engineering*, 2010, pp. 388–391, doi: 10.1109/EEEIC.2010.5489987.
- [3] J. Li, T. Jiang, and S. Grzybowski, "Hot spot temperature models based on top-oil temperature for oil immersed transformers," in *2009 IEEE Conference on Electrical Insulation and Dielectric Phenomena*, 2009, pp. 55–58, doi: 10.1109/CEIDP.2009.5377876.
- [4] A. Skillen, A. Revell, H. Iacovides, and W. Wu, "Numerical prediction of local hot-spot phenomena in transformer windings," *Applied Thermal Engineering*, vol. 36, pp. 96–105, Apr. 2012, doi: 10.1016/j.applthermaleng.2011.11.054.
- [5] M. T. Villén, J. Letosa, A. Nogués, and R. Murillo, "Procedure to accelerate calculations of additional losses in transformer foil windings," *Electric Power Systems Research*, vol. 95, pp. 85–89, Feb. 2013, doi: 10.1016/j.epr.2012.08.006.
- [6] W. Sun, L. Yang, D. Feng, X. Zhao, and J. Li, "A new accelerated thermal aging test for over-loading condition transformer," in *2016 IEEE Electrical Insulation Conference (EIC)*, Jun. 2016, pp. 354–357, doi: 10.1109/EIC.2016.7548612.
- [7] J. Niu, J. Su, Y. Yang, Y. Cai, and H. Liu, "Distribution transformer failure rate prediction model based on multi-source information," in *2016 International Conference on Condition Monitoring and Diagnosis (CMD)*, Sep. 2016, pp. 944–947, doi: 10.1109/CMD.2016.7757980.
- [8] N. Pandit and R. L. Chakrasali, "Distribution transformer failure in India root causes and remedies," in *2017 International Conference on Innovative Mechanisms for Industry Applications (ICIMIA)*, Feb. 2017, pp. 106–110, doi: 10.1109/ICIMIA.2017.7975582.
- [9] I. M. Sari, A. Tryollinna, A. D. P. Sudin, and D. Deka Permata, "Through fault current effects on distribution transformer and prevention actions using backup protection: Case study of Kelapa Gading transformer," in *2017 International Conference on High Voltage Engineering and Power Systems (ICHVEPS)*, Oct. 2017, pp. 247–251, doi: 10.1109/ICHVEPS.2017.8225951.
- [10] G. Liang, S. Li, R. Liu, J. Cao, Y. Hao, and W. Chen, "A probabilistic maintenance scheme evaluation method for transformer based on failure rate," in *2017 4th International Conference on Information Science and Control Engineering (ICISCE)*, Jul. 2017, pp. 90–93, doi: 10.1109/ICISCE.2017.29.
- [11] S. A. Deokar and L. M. Waghmare, "Impact of power system harmonics on insulation failure of distribution transformer and its remedial measures," in *2011 3rd International Conference on Electronics Computer Technology*, Apr. 2011, pp. 136–140, doi: 10.1109/ICECTECH.2011.5941817.
- [12] D. Cai, J. Tang, and J. Li, "The evaluation of thermal endurance of cast-resin dry-type transformer insulation structure," in *2012 China International Conference on Electricity Distribution*, Sep. 2012, pp. 1–4, doi: 10.1109/CICED.2012.6508446.
- [13] A. Borghetti et al., "A procedure to evaluate the risk of failure of distribution transformers insulation due to lightning induced voltages," in *22nd International Conference and Exhibition on Electricity Distribution (CIRED 2013)*, 2013, Art. no. 1484, doi: 10.1049/cp.2013.1258.
- [14] D. Flora S., M. K. Kumari, and J. S. Rajan, "A new approach to study the effects of copper sulphide on electric stress distribution in paper oil insulation of transformers," in *2014 IEEE Electrical Insulation Conference (EIC)*, Jun. 2014, pp. 198–202, doi: 10.1109/EIC.2014.6869375.
- [15] M. Dugalovski, K. Najdenkoski, and G. Rafajlovski, "Impact of current high order harmonic to core losses of three-phase distribution transformer," in *Eurocon 2013*, Jul. 2013, pp. 1531–1535, doi: 10.1109/EUROCON.2013.6625181.
- [16] M. Yazdani-Asrami, M. Mirzaie, and A. A. Shayegani Akmal, "No-load loss calculation of distribution transformers supplied by nonsinusoidal voltage using three-dimensional finite element analysis," *Energy*, vol. 50, pp. 205–219, Feb. 2013, doi: 10.1016/j.energy.2012.09.050.
- [17] D. Azizian, "Temperature prediction in cast-resin transformer due to non-linear loads," *Journal of Electrical Systems*, vol. 10, no. 4, pp. 238–249, 2014.
- [18] L.-M. Jiang, J.-X. Meng, Z.-D. Yin, Y.-X. Dong, and J. Zhang, "Research on additional loss of line and transformer in low voltage distribution network under the disturbance of power quality," in *2018 International Conference on Advanced Mechatronic Systems (ICAMEchS)*, Aug. 2018, pp. 364–369, doi: 10.1109/ICAMEchS.2018.8507080.
- [19] D. Wan, F. Qi, M. Zhao, L. Mao, X. Duan, and Y. Liu, "An improved method for calculating power transmission equipment loss and hot spot temperature in distribution network under harmonic disturbance," in *2019 IEEE 3rd Conference on Energy Internet and Energy System Integration (EI2)*, Nov. 2019, pp. 122–125, doi: 10.1109/EI247390.2019.9061860.
- [20] D. Wan, M. Zhao, X. Duan, H. Zhou, L. Mao, and K. You, "Life assessment study on distribution electric power transmission equipment based on harmonic modified hot spot temperature calculating model," in *2019 IEEE 3rd Conference on Energy Internet and Energy System Integration (EI2)*, Nov. 2019, pp. 138–141, doi: 10.1109/EI247390.2019.9061954.
- [21] I. Iskender and A. Najafi, "Evaluation of transformer performance under harmonic load based on 3-D time stepping finite element method," in *2014 16th International Conference on Harmonics and Quality of Power (ICHQP)*, May 2014, pp. 224–228, doi: 10.1109/ICHQP.2014.6842827.
- [22] J. Faiz, M. Ghazizadeh, and H. Oraee, "Derating of transformers under non-linear load current and non-sinusoidal voltage-an overview," *IET Electric Power Applications*, vol. 9, no. 7, pp. 486–495, Aug. 2015, doi: 10.1049/iet-epa.2014.0377.
- [23] A. Chidurala, T. Kumar Saha, and N. Mithulananthan, "Harmonic impact of high penetration photovoltaic system on unbalanced distribution networks-learning from an urban photovoltaic network," *IET Renewable Power Generation*, vol. 10, no. 4, pp. 485–494, Apr. 2016, doi: 10.1049/iet-rpg.2015.0188.
- [24] G. C. Jaiswal, M. S. Ballal, and D. R. Tutakne, "Impact of power quality on the performance of distribution transformer," in *2016 IEEE International Conference on Power Electronics, Drives and Energy Systems (PEDES)*, Dec. 2016, pp. 1–5, doi: 10.1109/PEDES.2016.7914344.
- [25] E. Cazacu, L. Petrescu, and V. Ionita, "Derating of power distribution transformers serving nonlinear industrial loads," in *2017 International Conference on Optimization of Electrical and Electronic Equipment (OPTIM) & 2017 Intl Aegean Conference on Electrical Machines and Power Electronics (ACEMP)*, May 2017, pp. 90–95, doi: 10.1109/OPTIM.2017.7974953.
- [26] R. Soni, P. Chakrabarti, Z. Leonowicz, M. Jasinski, K. Wiczorek, and V. Bolshev, "Estimation of life cycle of distribution transformer in context to furan content formation, pollution index, and dielectric strength," *IEEE Access*, vol. 9, pp. 37456–37465, 2021, doi: 10.1109/ACCESS.2021.3063551.
- [27] "IEEE guide for loading dry-type distribution and power transformers," in *IEEE Std C57.96-2013 (Revision of IEEE Std C57.96-1999)*, pp. 1–46, 27 Jan. 2014, doi: 10.1109/IEEESTD.2014.6725564."
- [28] COMSOL, "Heat transfer module," Manual, pp. 1–222, 2015."
- [29] "IEEE recommended practice for establishing liquid-filled and dry-type power and distribution transformer capability when supplying nonsinusoidal load currents," in *IEEE Std C57.110-2008 (Revision of IEEE Std C57.110-1998)*, pp. 1–52, Aug. 2008, doi: 10.1109/IEEESTD.2008.4601586.

BIOGRAPHIES OF AUTHORS

Muhammad Haziq Mohd Wazir    received the B.Eng. degree in electrical engineering from Universiti Teknologi Malaysia in 2021 in electrical engineering. Currently, he pursues PhD degree in Universiti Teknologi Malaysia in electrical engineering which includes renewable energy, power quality and electrical distribution system studies. He can be contacted at email: haziq@graduate.utm.my.



Dalila Mat Said    is an associate professor at the School of Electrical Engineering, Universiti Teknologi Malaysia (UTM). She has been with the Center of Electrical Energy Systems (CEES) since 2009. She received her B.Eng, M.Eng, and PhD degrees in electrical engineering from UTM in 2000, 2003, and 2012, respectively. She was involved in power quality consultancy for over 10 years and served as an energy auditor for the commercial and industrial sector. She is a senior member of the Institute Electrical Electronic Engineer (SMIEEE), registered as a graduate engineer with the Board of Engineers Malaysia (BEM) and an IEM graduate member as well as a Professional Technologist registered with the Malaysian Board of Technologies. Power quality and power system measurement and monitoring are her main areas of interest. She can be contacted at email: dalila@utm.my.



Zaris Izzati Mohd Yassin    is an electrical and electronics lecturer at the School of Engineering and Computing, Manipal International University (MIU). She received the B.Eng. and M.Eng. degrees in electrical engineering from Universiti Tun Hussein Onn Malaysia (UTHM) in 2012 and 2014, respectively, and the Ph.D. degree in electrical engineering from Universiti Teknologi Malaysia (UTM) in 2022. She has authored or coauthored journals and conference papers mainly related to power quality and electrical distribution networks. Her research interests include power quality monitoring, measurement and modelling for electrical power systems, distribution of electrostatic and magnetostatic fields using finite element method, and application of digital electronics. She can be contacted at email: zaris.izzati@miu.edu.my or zarisyassin@gmail.com.



Siti Aisyah Abd Wahid    is a research officer at the Centre of Electrical Energy Systems (CEES), Universiti Teknologi Malaysia (UTM). She received her B.Eng. and M.Eng. degrees in electrical engineering from UTM in 2008 and 2010 respectively. She has coauthored journals and conference papers mainly related to electrical distribution networks. She can be contacted at her email: staisyah@utm.my.